Spectrochimica Acta Part A 92 (2012) 336–346

Contents lists available at SciVerse ScienceDirect

Spectrochimica Acta Part A: Molecular and Biomolecular Spectroscopy

journal homepage: www.elsevier.com/locate/saa

Spectral, thermal and biological studies of Mn(II) and Cu(II) complexes with two thiosemicarbazide derivatives

Moamen S. Refat[a,b,*], Nashwa M. El-Metwaly[c,d]

[a] Department of Chemistry, Faculty of Science, Port Said University, Port Said, Egypt
[b] Department of Chemistry, Faculty of Science, Taif University, Taif 888, Saudi Arabia
[c] Department of Chemistry, Faculty of Science of Girls, Abha, King Khalid University, Saudi Arabia
[d] Department of Chemistry, Faculty of Science, Mansoura University, Egypt

ARTICLE INFO

Article history:
Received 15 November 2011
Received in revised form 4 February 2012
Accepted 10 February 2012

Keywords:
Spectral
Thermal
Biological
Thiosemicarbazide derivatives

ABSTRACT

Two derivatives of thiosemicarbazide were prepared. Their complexes were prepared using Mn(II) and Cu(II) salts. All the isolated complexes are characterized using the following spectra: IR, UV–Vis, Mass, ^{1}H NMR and X-ray diffraction. Magnetic measurements and thermal analysis are the other additive tools for complete investigation. Mononuclear and binuclear complexes are proposed based on elemental analysis mainly. The IR spectra offer the mode of coordination of each ligand with each metal ion. The electronic spectra and magnetic measurements are proposing the structural geometry of the investigated complexes. The octahedral geometry proposed for Mn(II) complexes but the square–planar for Cu(II) complexes. The ^{1}H NMR spectra were done for all organic compounds used in this study and displaying the most suitable tautomer of them. X-ray diffraction of H_2L^1 and its complexes show their amorphous nature but H_2L^2 ligand and its complexes show their nanocrystalline nature. The TG analysis was used to prove the presence of solvent molecules attached with the complexes as covalently or physically. Finally, the biological investigation was carried out for H_2L^2 ligand and its complexes and displaying the inhibition activity of Cu(II) complex than the Mn(II) one.

1. Introduction

The compounds containing thione (C=S) and thiole (C—S) groups occupy an important position among organic reagents as potential donor ligands for transition metal ions [1]. Both the organic compounds and their metal complexes display a wide range of pharmacological activity including anticancer antibacterial and fungi static effects. Thiosemicarbazones usually act as chelating ligands with transition metal ion, bonding through the sulphur and hydrazine nitrogen atoms. Also, compounds containing O, S and N atoms and their complexes have received considerable attention because of their pharmacological activities [2]. The metal complexes show more activities as compared to the free thiosemicarbazides. They show numerous applications [3–5] particularly with the first row of transition metal complexes. In view of above applications it is highly desirable to synthesize and characterize transition metal complexes with such ligands. The structure of the thiosemicarbazide moiety confers a good chelating capacity and this property can be increased in thiosemicarbazone by inserting suitable aldehyde or ketone possessing further donor atoms to render the ligand polydentate [6]. The variety of possible Schiff bases metal complexes with wide choice of ligands and coordination environments has prompted us to undertake research in this area [7]. In the present work we report the synthesis and characterization of Mn(II) and Cu(II) complexes with two thiosemicarbazide derivatives from 5-bromo-2-hydroxybenzaldehyde and 2-hydroxybenzaldehyde. This is to gain more information about related structural and spectral properties as well as their antimicrobial activities which are shining from the literature for similar compounds especially with Cu(II) and Mn(II).

2. Experimental work

2.1. Materials

All the chemicals used are of analytical grade. Organic chemicals such as phthalic anhydride, thiosemicarbazide and 5-bromo-2-hydroxybenzaldehyde or 2-hydroxybenzaldehyde were purchased from Fluka Chemical Co., $MnCl_2{\cdot}4H_2O$ and $CuCl_2{\cdot}2H_2O$ from (Merck Co.).

---

* Corresponding author at: Department of Chemistry, Faculty of Science, Port Said University, Port Said, Egypt. Tel.: +966 561926288.
E-mail address: msrefat@yahoo.com (M.S. Refat).

1386-1425/$ – see front matter © 2012 Elsevier B.V. All rights reserved.
doi:10.1016/j.saa.2012.02.041

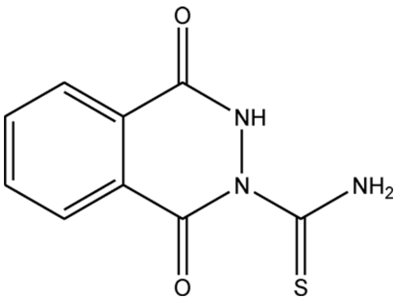

Fig. 1. 1,4-Dioxo-3,4-dihydrophthalazine-2(1*H*)-carbothioamide (H_2DDCA).

2.2. Synthesis of thiosemicarbazide derivative (H_2DDCA)

A mixture of phthalic anhydride (0.01 mol) and thiosemicarbazide (0.01 mol) in acetic acid (30 ml) was heated under reflux for 2–3 h, then cooled. The solid product formed was filtered off, washed with ethanol, dried and purified by recrystallization from acetic acid to give as colorless crystals (Fig. 1), yield 87%.

2.3. Synthesis of H_2L^1 and H_2L^2 ligands

A mixture of ethanolic solution (30 ml) of H_2DDCA (0.01 mol) with 0.01 mol of each aldehyde was heated under reflux for 2–3 h. The solid product formed was filtered off, washed with ethanol, dried and purified by recrystallization from ethanol and separated as white crystals (Fig. 2a and b).

2.4. Synthesis of metal ion complexes

A mixture of hot ethanolic solution (10 ml) of free ligand (0.002 mol) and hot ethanolic solution (10 ml) of (0.002 ml) each metal ion salt was refluxed for 3–4 h at 70–80 °C. The resulting solutions are allowed to stand, a brown colored crystals of Cu(II) complexes were aggregated. The same color crystals of Mn(II) complexes were appeared after adjusting the pH at ≈6 using drops of diluted ammonia solution. The crystals are filtered off, washed with ethanol and deride over $CaCl_2$. The purity of the complexes was checked by TLC.

2.5. Physical measurements

Carbon and hydrogen contents were determined using a Perkin-Elmer CHN 2400 in the Micro-analytical Unit at the Faculty of Science, Cairo University, Egypt. The metal content was determined using complexometric titrations and the Cl was tested gravimetrically using $AgNO_3$ [8]. IR spectra were recorded on a Mattson 5000 FTIR Spectrophotometer (4000–400 cm^{-1}) using KBr pellets. The UV–Vis, spectra were determined in the DMSO solvent with concentration (1.0×10^{-3} M) for the free ligands and their complexes using Jenway 6405 Spectrophotometer with 1 cm quartz cell, in the range 200–800 nm. Molar conductance were measured using Jenway 4010 conductivity meter for the freshly prepared solutions at 1.0×10^{-3} mol in DMSO solvent. Magnetic measurements were carried out on a Sherwood Scientific magnetic balance in the Micro Analytical Laboratory, Faculty of Science, Mansoura University, Egypt, using Gouy method. Calibration: two very good solid calibrants are used: $Hg[Co(CNS)_4]$ and $[Ni(en)_3](S_2O_3)$. They are easily prepared in pure state, do not decompose or absorb moisture and pack well. Their susceptibilities at 20 °C are 16.44×10^{-6} and 11.03×10^{-6} c.g.s. Units, decreasing by 0.05×10^{-6} and 0.04×10^{-6} per degree temperature raise respectively, near room temperature. The cobalt compound, besides having the higher susceptibility, also packs rather densely and is suitable for calibrating low fields, while the nickel compound with lower susceptibility and density is suitable for higher field [4]. Here we are used $Hg[Co(CNS)_4]$ only as calibrant. ^{1}H NMR spectrum of the organic compounds were recorded on Varian Gemini 200 MHz spectrometer using DMSO-d_6 as solvent. The electron-impact mass spectra of the free ligands and two of their complexes were checked at 70 eV using AEI MS 30 Mass spectrometer. The X-ray powder diffraction analyses were carried out using Rigku Model ROTAFLEX Ru-200 with copper target. Thermogravimetric and its differential analysis (TGA/DTG) were carried out in dynamic nitrogen atmosphere (30 ml/min) with a heating rate of 10 °C/min using a Shimadzu TGA-50H thermal analyzer. The biological activity screening was tested in Micro Analysis Laboratory in Alixanderia University.

2.6. Antibacterial antifungal screening

In vitro antibacterial screening is performed by the agar disc diffusion method [9]. The species used in the screening are; gram-negative bacteria as: *Escherishia coli* sp. and *Pesudomonas* sp. And gram-positive bacteria as: *Bacillus subtilis*, *Streptococcus pneumonia* and *Staphylococcus aureas*. Fungi as: *Aspergillus nigaer* and *Penicillium* sp. Stock cultures of the tested organisms are maintained on nutrient agar media by sub culturing in Petri dishes. The media are prepared by adding the components as per manufacturer's instructions and sterilized in the autoclave at 121 °C and atmospheric pressure for 15 min. Each medium is cooled to 45–60 °C and 20 ml of it, is poured into a Petri dish and allowed to solidify. After solidification, petri plates with media are spread with 1.0 ml of bacterial or fugal suspension prepared in sterile distilled water. The wells are bored with cork borer and the agar plugs are removed. To each agar well, unique concentration of 100 μg for each compound in DMF (75 μl) were applied to the corresponding well (6 mm). All the plates are incubated at 37 °C for 24 h and they are observed for the growth inhibition zones. The presence of clear zones around the wells indicate that the ligand and its complexes are active. The diameter of zone of inhibition is calculated in millimeters. The well diameter is deducted from the zone diameter and the values are tabulated.

3. Results and discussion

The isolated complexes are stable in air, insoluble in water and common organic solvents, but are completely soluble in DMSO and DMF. Mn(II)–H_2L^1, Cu(II)–H_2L^1 and Mn(II)–H_2L^2 complexes having high m.p. (300, 280 and 250 °C, respectively) than the free ligands (≈220 °C) but the Cu(II)–H_2L^2 having low m.p. (180 °C). The elemental analysis (C, H M and Cl), color and formula weights are listed in Table 1. The Cl was tested gravimetrically for the Mn(II)–H_2L^2 and Cu(II)–H_2L^2 complexes due to the absence of Br from the ligand structure which its presence cause a higher difference in between the found and calculated percentage proposed due to its precipitation with $AgNO_3$. Attempts to propose the structures of the isolated complexes come from full investigation as the following studies.

3.1. IR spectra and mode of bonding

The IR spectral data containing the relevant vibrational bands of the Cu(II) and Mn(II) complexes are listed in Table 2. The IR spectrum of free H_2L^1 ligand shows a medium intense absorption bands at 3452 and 1351 cm^{-1} due to υ and δ(OH), respectively. The bands appear at 1475, 1262, 1122 and 771 cm^{-1} were assigned to thioamide I, II, III and IV vibrations [10,11], respectively. Further, the ligand is expected to undergo keto, thione ↔ enol, thiol tautomerism. However, the appearance of four thioamide bands in ligand indicates the existence of the ligand in the keto, thione form. The intense band at 1544 cm^{-1} assigned for the interaction

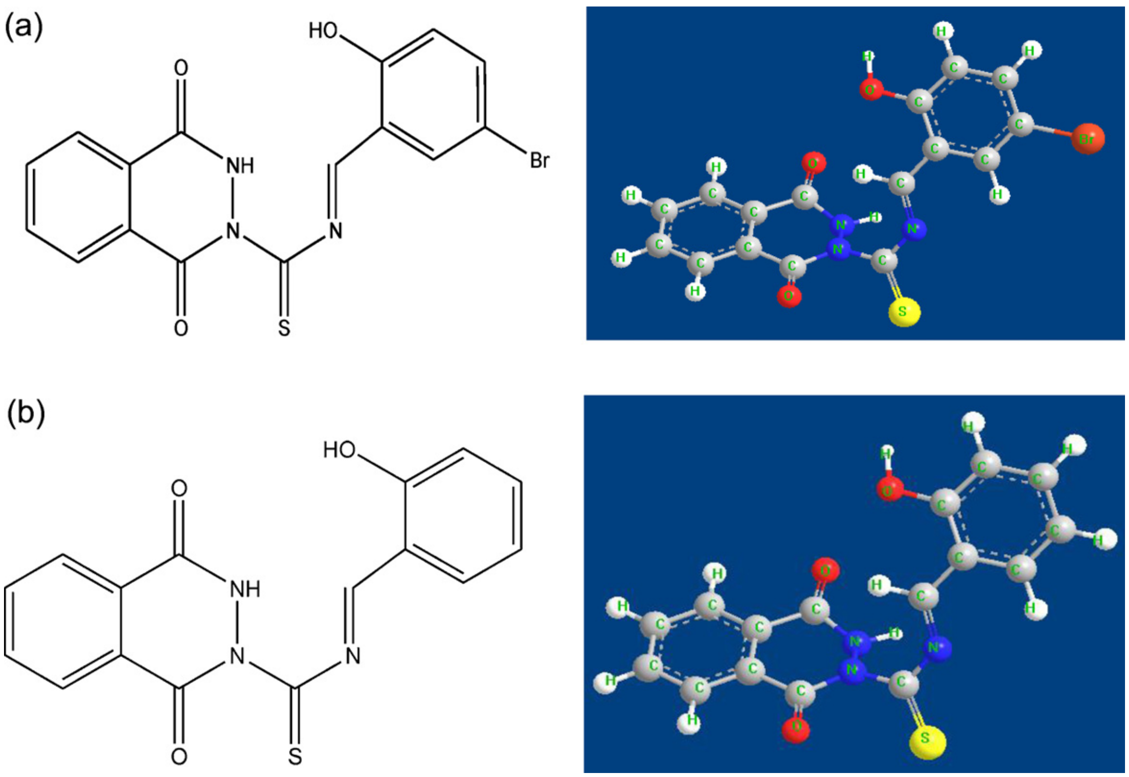

Fig. 2. (a) (*E*)-*N*-(5-bromo-2-hydroxybenzylidene)-1,4-dioxo-3,4-dihydrophthalazine-2(1*H*)-carbothioamide(H_2L^1). (b) (*E*)-*N*-(2-hydroxybenzylidene)-1,4-dioxo-3,4-dihydrophthalazine-2(1*H*)-carbothioamide (H_2L^2).

Table 1
Analytical and physical data for H_2L^1 and H_2L^2 ligands and their metal complexes.

Compound Empirical formula (M.Wt.)	Color	Ω^2 cm^{-1} mol^{-1}	Elemental analysis (%) calcd. (found)			
			C	H	M	Cl
(1) [$C_{16}H_{10}N_3SO_3Br$] (H_2L^1) (404.24)	White	–	47.54 (47.55)	2.49 (2.48)	–	–
(2) [$MnCl_3{\cdot}3(H_2O)(C_{16}H_9N_3SO_3Br)$] (673.51)	Brown	18	28.53 (28.55)	2.24 (2.22)	16.31 (16.32)	–
(3) [$CuCl_2(C_{16}H_{10}N_3SO_3Br)$] (538.69)	Brown	15	35.67 (35.64)	1.87 (1.88)	11.79 (12.0)	–
(4) [$(C_{16}H_{11}N_3SO_3)$](H_2L^2) (325.35)	White	–	59.07 (59.02)	3.41 (3.44)	–	–
(5) [$MnCl_2{\cdot}H_2O(C_{16}H_{11}N_3SO_3)$] (469.19)	Brown	24	40.96 (40.97)	2.79 (2.77)	11.71 (11.71)	15.11 (15.10)
(6) [$Cu_2Cl_2(C_{16}H_{11}N_3SO_3)$]2Cl·$H_2O$ (612.27)	Brown	117	31.39 (31.39)	2.14 (2.14)	20.76 (20.77)	23.16 (23.16)

Table 2
Assignments of essential IR spectral bands (cm^{-1}) of H_2L^1 and H_2L^2 ligands and their metal complexes.

Compound	υ_{OH}	υ_{NH}	$\upsilon_{C=N}$	$\upsilon_{C=O(amide)}$	δ_{OH}	δ_{NH}	$\upsilon_{IV(C=S)}$	υ_{M-S}	υ_{M-N}	υ_{M-O}
(1) [$C_{16}H_{10}N_3SO_3Br$] (H_2L^1)	3452	3249	1544	1607	1351	1544	771	–	–	–
(2) [$MnCl_3{\cdot}3(H_2O)(C_{16}H_9N_3SO_3Br)$]	3425	3154	1525	1596	1365	1562	750	410	444	548
(3) [$CuCl_2(C_{16}H_{10}N_3SO_3Br)$]	3452	3256	1544	1603 1590	1354	1544	726	431	–	559
(4) [$(C_{16}H_{11}N_3SO_3)$] (H_2L^2)	3443	3319	1538	1613	1365	1489	774	–	–	–
(5) [$MnCl_2{\cdot}H_2O(C_{16}H_{11}N_3SO_3)$]	3441	3286	1538	1600 1590	1323	1467	732	414	441	553
(6) [$Cu_2Cl_2(C_{16}H_{11}N_3SO_3)$]2Cl· H_2O	3449	3321	1540	1601	1360	1492	732	409	478	584

of υ(C=N) and δ(NH) bands. Also, an intense band at 1607 cm^{-1} assigned for υ(C=O) of two similar amide groups. A deliberate comparison between the spectra of investigated complexes with the spectrum of free ligand reflects the mode of coordination of the ligand towards metal ions. The IR spectrum of Mn(II)–H_2L^1 complex shows the following bands suffer shifts in appearance due to the coordination of all active sites. A broad band at ≈3425 cm^{-1} assigned to υOH of coordinated water molecules although the proposal of deprotonation of OH group in the ligand molecule during its covalent attachment with one central atom. The lower shift of υNH band and the thioamide bands especially the fourth υ(C=S) (750 cm^{-1}) proposed their participation in coordination. Also, the lower appearance of a band at 1525 cm^{-1} assigned for υ(C=N) group offers the fourth coordination site. The lower appearance of intense υ(C=O) bands at 1596 cm^{-1} offers the fifth and sixth coordination sites. The binuclear presence of Mn(II) permit the coordination of all active sites of the ligand which shows a mononegative polydentate mode towards the two central atoms. The IR spectrum of Cu(II)–H_2L^1 complex displays the following more or less unshifted bands: 3452, 3256 and 1603 assigned for υOH, υNH and υ(C=O). The appearance of new band at 1590 cm^{-1} assigned for the coordinated C=O group in-between the two amides in phthalic anhydride. Also, the lower shift observed with υ(C=S) bands proposed its interaction with central atom by a coordinate bond. The ligand coordinates towards Cu(II) as neutral bidentate through C=O and C=S groups. The different interaction mode of the H_2L^1 towards Cu(II) and Mn(II), due to the different coordination media pH. The use of ammonia drops to isolated the Mn(II) complex facilitate the ionization of the ligand through OH group during the coordination. The IR spectrum of H_2L^2 ligand displays the following significant bands at: 3443, 3319, 1489, 1365, 1538 and 1613 cm^{-1} assigned for υOH, υNH, δNH, δOH, υC=N and υC=O. Also, other additive bands at 1464, 1267, 1110 and 774 cm^{-1} for thioamide group. This appearance also, supports the presence of the free ligand in keto-thione form. The IR spectrum of Mn(II)–H_2L^2 complex displays the same significant bands suffer little affect although the proposal of their ruling out from coordination with central atom as: 3441, 3286, 1600 and 1538 cm^{-1} assigned for υOH, υNH, υC=O and υC=N. The bands suffer changes in their position at 1490, 1292, 1120 and 732 cm^{-1} assigned for thioamide group coordinated with central atom. This is proven through the higher appearance of first three bands but the lower appearance of the fourth is considered the major measure of C=S coordination. The appearance of new band at 1590 cm^{-1} assigned for coordinated C=O group in between two amides. The ligand coordinates towards Mn(II) as neutral tridentate through one amide and C=S groups. The spectrum of Cu(II)–H_2L^2 complex displays these bands at 3449, 3321, 1492 and 1540 cm^{-1} assigned for υOH, υNH, δNH and υC=N bands which suffer higher and lower shift. Other bands at 1469, 1260, 1128 and 732 cm^{-1} for stretching thioamide bands suffer little lower shift except the fourth suffers a strong lower shift coherently with the proposal of its coordination. The ligand coordinates towards two Cu(II) as neutral polydentate mode through all its active sites. The lower appearance of all significant bands in the two free ligands (H_2L^1 and H_2L^2) may reflect the presence of intraligand H-bonding which, is normally found especially with the presence of condensed highly electronegative sites. Also, a higher or a little lower shift observed with some bands assigned for groups sometimes are completely sided from coordination media due to the decomposition of intra ligand H-bonding during the coordination only. The new bands appeared in lower frequency region assigned for M–L bands with O, N and S atoms are well characterized. The M–Cl cannot easily detect in this scanning range but proposed based on elemental analysis and conductivity measurements.

3.2. Molar conductivity measurements

The molar conductivity values of Mn(II)–H_2L^1, Cu(II)–H_2L^1 and Mn(II)–H_2L^2 complexes (Table 1) were found to be in the range of 15–24 Ω^2 cm^{-1} mol^{-1}. These relatively low values indicate the non-electrolytic nature of these complexes [12]. The neutrality of the complexes can be accounted by both the deprotonated nature of the ligand with most complexes and the attaching of Cl covalently the metal ions. The Cu(II)–H_2L^2 complex is the only displaying higher conductivity value (117 Ω^2 cm^{-1} mol^{-1}) referring to 1:2 electrolyte in between the coordination sphere and the chloride ions [13].

3.3. Electronic spectra and magnetic measurements

A comparison of the electronic spectra of the free ligands with those of their corresponding metal complexes show some shifts that can be considered as evidence for the complex formation. These bands appeared in neutral medium for the free ligands at ≈350 and ≈270 nm. These bands may be attributed to $n \rightarrow \pi^*$ and $\pi \rightarrow \pi^*$ transitions inside the ligands function groups. Additionally, the absorption spectra (in DMSO) of metal complexes show additive bands at different wave lengths. Each one is corresponding to certain transition, which suggests the geometry of the complexes and supported by the magnetic susceptibility values. The tentative assignments of the significant electronic spectral absorption bands of H_2L^1 and H_2L^2 with their Mn(II) and Cu(II) complexes as well as their μ_{eff} values are given in Table 3. The absorption spectra of Mn(II)–H_2L^1 and Mn(II)–H_2L^2 complexes display weak absorption bands at; 22,222, 27,778 and 34,482 also; 21,739, 28,571 and 35,088 cm^{-1} in each complex, respectively are characteristic for octahedral geometry (Fig. 3). These bands may be assigned as $^6A_{1g} \rightarrow {}^4E_{1g}$, $^4A_{1g}(^4G)$, $^6A_{1g} \rightarrow {}^4E_g(^4D)$ and $^6A_{1g} \rightarrow {}^4T_{1g}(^4P)$ transitions, respectively [14,15]. According to the d^5 electronic configuration of Mn(II) an effective magnetic moment for high spin complexes is expected to be 6.0 BM. Measured magnetic moments (Table 3) are 5.86 and 5.88 BM confirm the octahedral environment for the Mn(II) with five unpaired electrons in the two complexes. The electronic spectra of Cu(II)–H_2L^1 and Cu(II)–H_2L^2 complexes exhibit two bands as; an asymmetric broad band at 16,666 and 15,285 cm^{-1}, respectively and a more intense band at 22,222 and 24,390 cm^{-1}. The latter band may be assigned to ligand–metal charge transfer transition. The asymmetric band is assigned to the transition $^2T_{2g} \rightarrow {}^2E_g$. The band position and the magnetic moment values (1.76 and 1.02 BM) can be taken as evidence for the square–planar configuration (Fig. 3) [16]. The first value (1.76 BM) was found in the usual range for d^9 system and indicating no direct interaction between central atoms in neighboring molecules, but the second one (1.02 BM) is lower than normal. This is may be due to a strong interaction between the two central atoms contribute in the same complex nucleus.

3.4. ^{1}H NMR spectra of organic compounds

A literature survey reveals that the NMR spectroscopy has been proved useful in establishing the structure and nature of many ligands and their diamagnetic complexes. The ^{1}H NMR spectra (Fig. 4a–c) were recorded in d_6-dimethylsulfoxide (DMSO-d_6) solution using Me_4Si (TMS) as internal standard. The proton magnetic resonance spectrum of H_2DDCA shows the existence of it in its enolic form. This may be due to the higher polarity over the hall molecule. ^{1}H NMR (ppm) δ = 2.50 (DMSO); 7.40–8.20 (m, 4H, C_6H_4); 9.40 (s, 2H, NH_2) and 10.4 ppm (s, 1H, OH). The ^{1}H NMR spectra of H_2L^1 and H_2L^2 ligands show a singlet signals at δ = 11.42 and 11.39 ppm due to OH [17] and signals at δ = 10.23 and 9.89 ppm (s, 1H) can be assigned to NH proton. The multiplets at δ = 6.79–8.31

Table 3
Magnetic moments (BM) and electronic spectral bands (cm^{-1}) of the complexes.

Complex	μ_{eff} (BM)	d–d transition (cm^{-1})	Intraligand and charge transfer (cm^{-1})
(2) $[MnCl_3{\cdot}3(H_2O)(C_{16}H_9N_3SO_3Br)]$	5.86	22,222; 27,778	28,560; 34,482; 37,001
(3) $[CuCl_2(C_{16}H_{10}N_3SO_3Br)]$	1.76	16,666; 15,285	27,900; 36,496
(5) $[MnCl_2{\cdot}H_2O(C_{16}H_{11}N_3SO_3)]$	5.88	21,739; 28,571	35,088; 36,765
(6) $[Cu_2Cl_2(C_{16}H_{11}N_3SO_3)]2Cl{\cdot}H_2O$	1.02	22,222; 24,390	36,496; 28,560

and 6.78–8.39 ppm ranges assigned to phenyl protons (m, 7H) and (m, 8H), respectively. While, the signal at $\delta = 3.35$ and 3.48 ppm (s, 1H) of CH proton. Also, singlet signals at $\delta = 2.51$ and 2.52 ppm for DMSO solvent.

3.5. X-ray powder diffraction of the ligands and their complexes

X-ray powder diffraction pattern in the $\theta < 2\theta < 60°$ of the ligands and their Mn(II) and Cu(II) complexes were carried out in order to give an insight about the lattice dynamics of these compounds. The X-ray powder diffraction obtained reflects a shadow on the fact that each solid represents a definite compound of a definite structure which is not contaminated with starting materials. Such facts suggest that the H_2L^1 ligand and its complexes are amorphous in nature but H_2L^2 ligand and its complexes reveal their nanocrystalline nature (Fig. 5) which identified through a smoothly peaks observed.

3.6. Molecular modeling

An attempt to gain a better insight on the molecular structure of the ligand and its complexes geometry optimization and conformational analysis has been performed by the use of MM^+ [18] force field as implemented in hyperchem 7.5 [19]. The drown modeling structures of the free ligands display the stable stereo structure includes the lowest energy level (total energy 18.156 of H_2L^1 and total energy = 17.907 kcal/mol of H_2L^2) in between others may be proposed. This arrangement of sites welling to coordination may support the mode of coordination proposed in the investigated complexes.

3.7. Mass spectral analysis

The mass spectra of all organic compounds and some complexes (Cu(II)–H_2L^1 and Mn(II)–H_2L^2) have been recorded. The purity of H_2DDCA compound was evaluated using microanalysis mass spectra (Fig. 6 as ex.). Where, the spectrum showed an essential peak attributed to molecular ion peak ($m/z = 221$) confirming that theoretically proposed. The fragmentation pathway of the compound is presented in Scheme 1, ended with the assignment for the base peak. The spectrum of H_2L^1 shows a well defined parent peak at $m/z = 403$ (Calcd. 404.24) for M^+ with a moderate intensity (29%). The parent ion peak and the fragmentation pathway obtained through cleavage in different positions in the molecule are shown in Scheme 2. The mass spectrum of its Cu(II) complex does not display a peak refers to molecular ion peak. This may reflecting the sudden fragmentation during the evaporation process. I think a cleavage happened to an organic part surrounds the metal ion. The first peak at $m/z = 275$ by 71.1% intensity which is higher intensity than known for molecular ion peak, which is usually in a moderate intensity, such may support our imagination. The lower intensity gives an idea of stability of the fragment except the base peak.

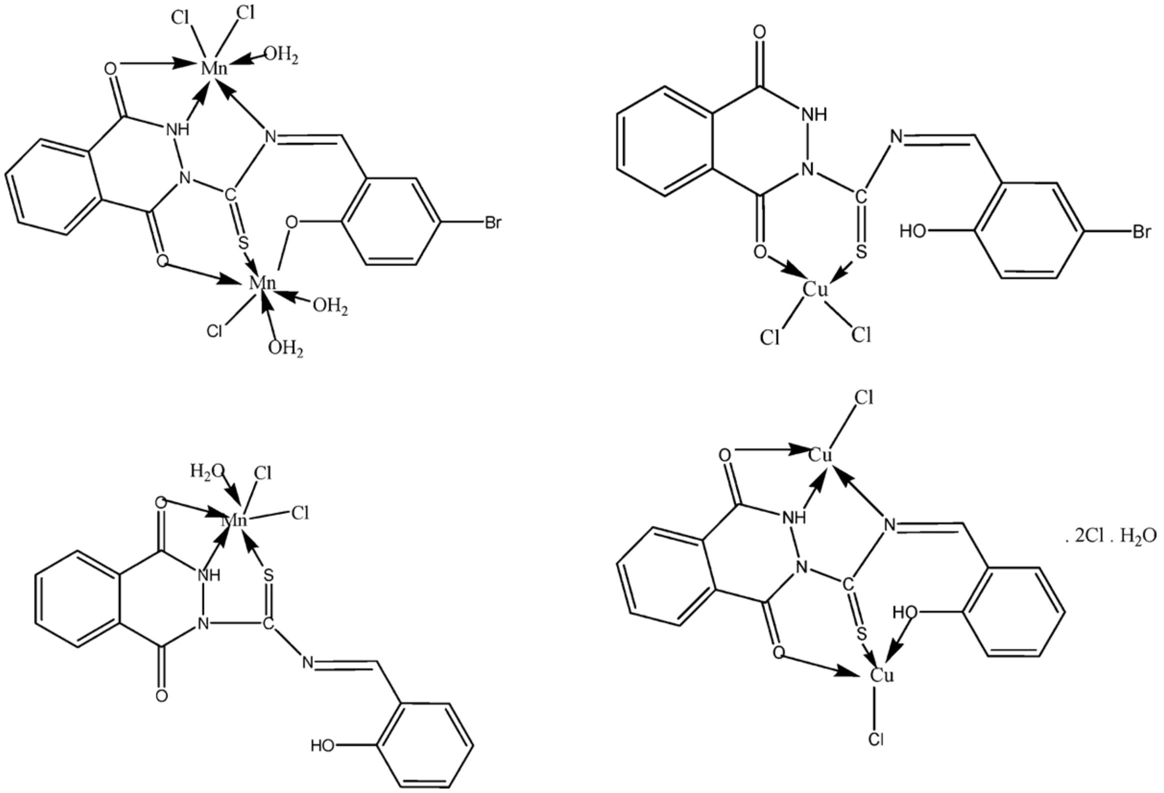

Fig. 3. The proposed structures of the investigated complexes.

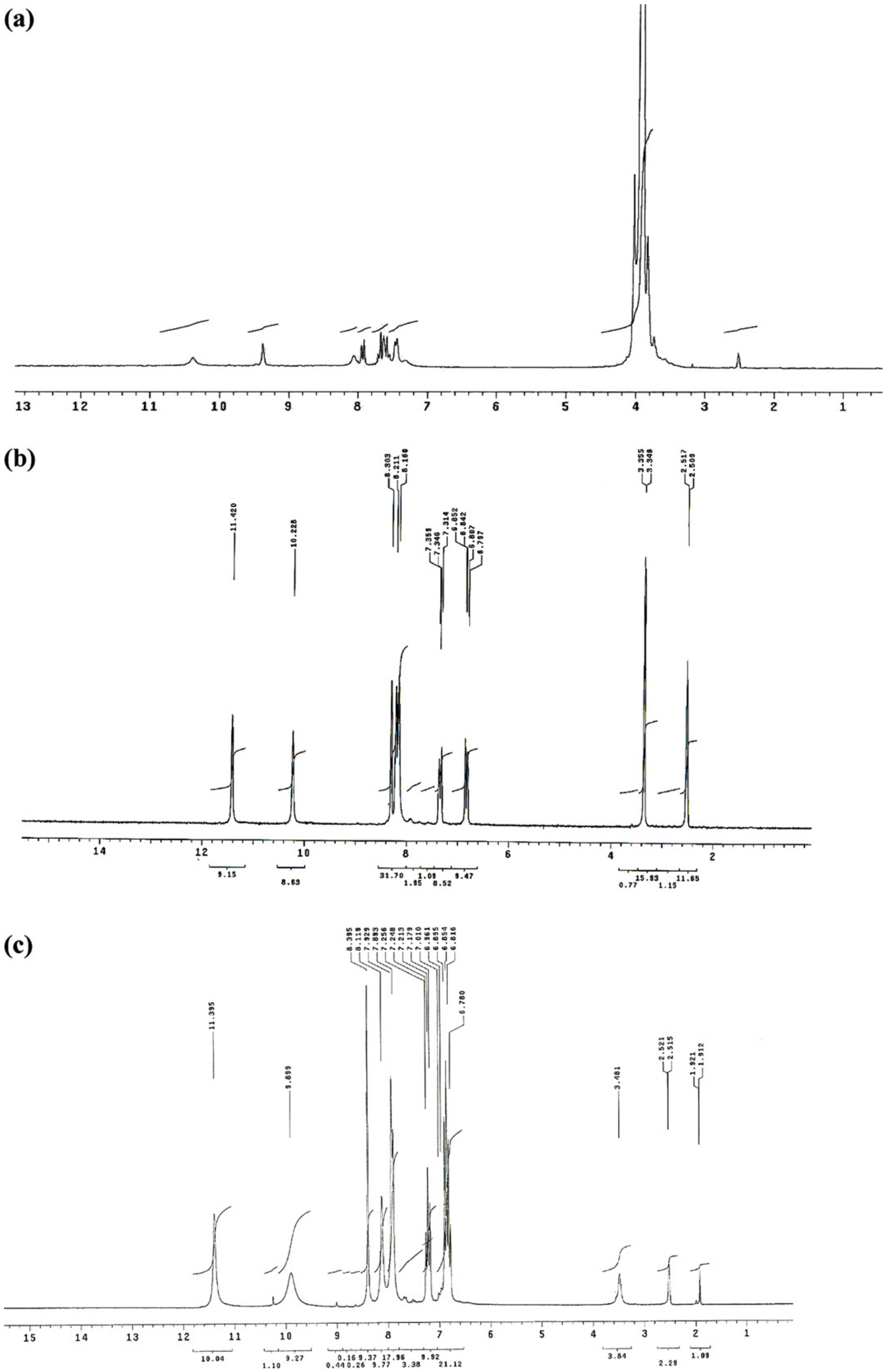

Fig. 4. The ^{1}H NMR spectra of (a) H_2DDCA, (b) H_2L^1 and (c) H_2L^2 ligands.

The base peak at $m/z = 63$ (the final fragment at $m/z = 60$) may be attributed to Cu ion. Also, the lower m.p. (180 °C) of the complex goes in a parallel with its behavior in mass spectral analysis reflecting the relative instability nature. This spectrum is not used at all as a further support for the molecular formula for this complex, but the base peak assigned for one Cu(II) ion supports the mononuclear complex proposed. The mass spectrum of H_2L^2 ligand displays a well defined peak at $m/z = 308$ (Calcd. = 325.34) by 35% intensity. This is may be strongly attributed to $[M-OH]^+$. The other following peaks assignable for various fragments arising from the cleavage of

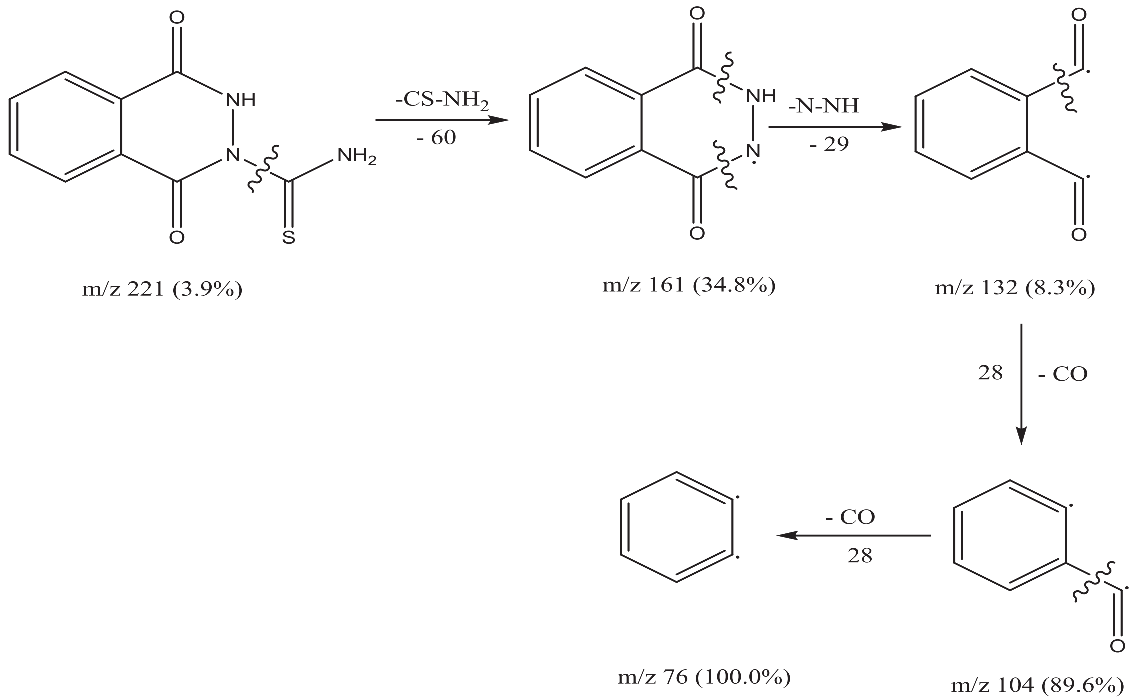

Scheme 1. The fragmentation pattern of H_2DDCA compound.

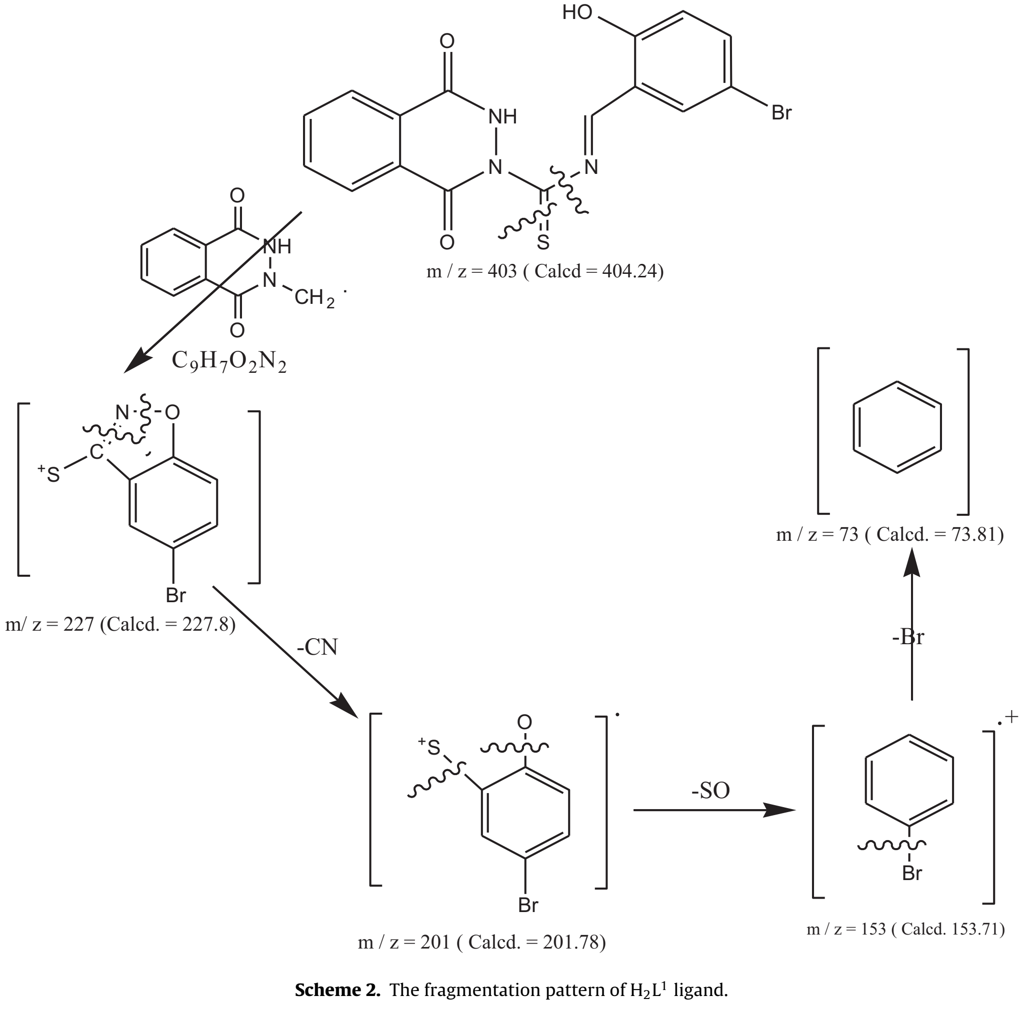

Scheme 2. The fragmentation pattern of H_2L^1 ligand.

the compound. The base peak at *m*/*z* = 52 (Calcd. 52.08) is assignable for C_4H_4. The mass spectrum of its Mn(II) complex shows a parent peak at *m*/*z* = 450 (Calcd. 469.19) by 43% intensity. This peak may be attributed to M^+-H_2O, which somewhat happened especially with the presence of solvent molecules attached with the metal ion, such molecules may be easily repelled during the evaporation of the complex in an introductory step for the analysis. The base peak appeared at *m*/*z* = 198 (Calcd. 198.06). This peak may be attributed to Mn surrounds with a part of organic compound as $MnC_3HN_3SO_2$. This peak is followed by other fragmentation peaks by lower intensity.

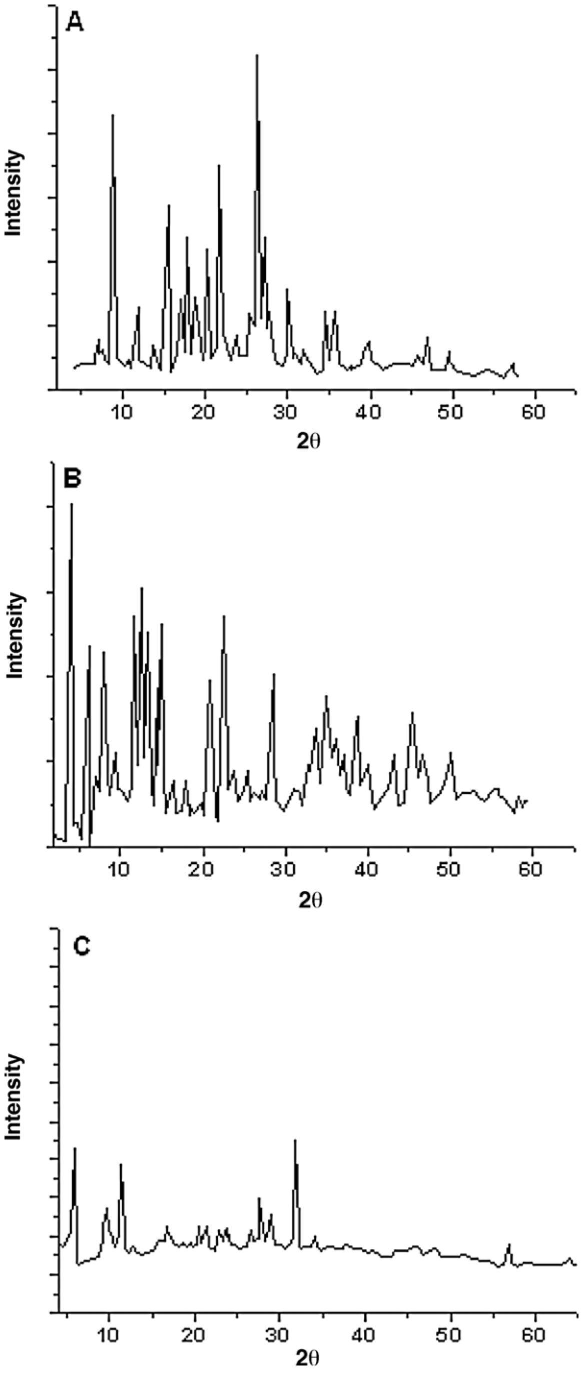

Fig. 5. XRD spectra of (A) H_2L^2 ligand, (B) Cu(II)–H_2L^2 and (C) Mn(II)–H_2L^2 complexes.

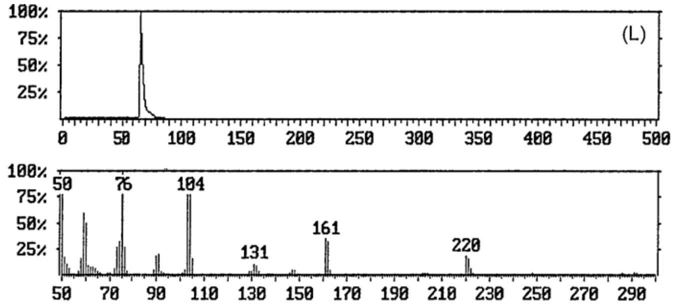

Fig. 6. The mass spectrum of H_2 DDCA compound.

Table 4
Thermogravimetric analysis data of the investigated complexes.

Complex	Steps	Temp. range (°C)	Decomposed assignments	Weight loss Found (calcd. %)
(2)	1st	150–330	$-C_7H_5ONBr + 3H_2O$	38.15 (37.57)
	2nd	330–475	$-1.5Cl_2$	15.04 (15.79)
	3rd	475–800	$-C_9H_4NO_2$	23.91 (23.48)
	Residue		MnN + MnS	22.89 (23.15)
(3)	1st	100–190	$-0.5Cl_2$	6.07 (6.58)
	2nd	190–250	$-C_6H_4$	13.73 (14.12)
	3rd	250–360	−ClBr + CO	25.81 (26.60)
	4th	360–800	$-C_5H_6N_3O_2$	26.01 (26.87)
	Residue		CuS + 4C	27.56 (26.67)
(5)	1st	50–217	$-H_2O + C_6H_5O$	23.10 (23.68)
	2nd	217–365	$-C_6H_4 + O_2$	23.14 (23.04)
	3rd	365–655	$-0.5N_2 + Cl_2$	18.30 (18.09)
	4th	655–800	$-N_2 + H_2$	6.91 (6.40)
	Residue		MnS + 4C	28.53 (928.78)
(6)	1st	46–170	$-H_2O$	2.44 (2.94)
	2nd	170–300	$-C_{12}H_8 + Cl_2$	37.72 (36.44)
	3rd	300–420	$-C_2H_3O_2$	9.11 (9.64)
	4th	420–448	$-1.5N_2$	6.24 (6.86)
	5th	448–800	$-Cl_2$	11.96 (11.58)
	Residue		CuO + CuS + 2C	32.56 (32.53)

3.8. Thermogravimetric analysis

Thermogravimetric studies (TG) for the complexes were carried out within the temperature range from room temperature up to 800 °C. TG results are in good agreement with the suggested formula resulted from microanalysis data (Table 1). The determined temperature ranges and percent mass losses of the solid complexes on heating are given in Table 4. The data reveal the following findings: the Mn(II)–H_2L^1 complex was thermally decomposed at 150–800 °C range. The first decomposition step of estimated mass loss 38.15% (Calcd. Mass loss 37.57%) within the temperature range 150–330 °C may be attributed to the liberation of $3H_2O$ molecules beside an organic part (C_7H_5ONBr). The energy of activation in this step was 1200 kJ mol^{-1}. The second and third steps found within the range 330–800 °C with an estimated mass loss 38.95 (Calcd. Mass loss 39.27%) which are responsibly accounted for the removal of 1.5 Cl_2 molecules along with the decomposition of the rest organic part with a final of MnN + MnS. The TG curve of Cu(II)–H_2L^1 complex showed four closed steps. The first estimated mass loss of 6.07% within the range of 100–190 °C (Calcd. Mass loss 6.58%) may be attributed to the loss of 0.5 Cl_2 molecule. The second and third steps found within the range 190–360 °C with an estimated mass loss 39.54 (Calcd. Mass loss 40.72%) and may attributed to the loss of C_6H_4 and CO + ClBr molecules. The final step ended at 800 °C with an estimated mass loss of 26.01% (Calcd. Mass loss = 26.87%) corresponding to the loss of remaining organic part ($C_5H_6N_3O_2$). The final residue is CuS polluted with 4C atoms. The TG curve of Mn(II)–H_2L^2 complex was thermally decomposed in four definite successive decomposition steps. The

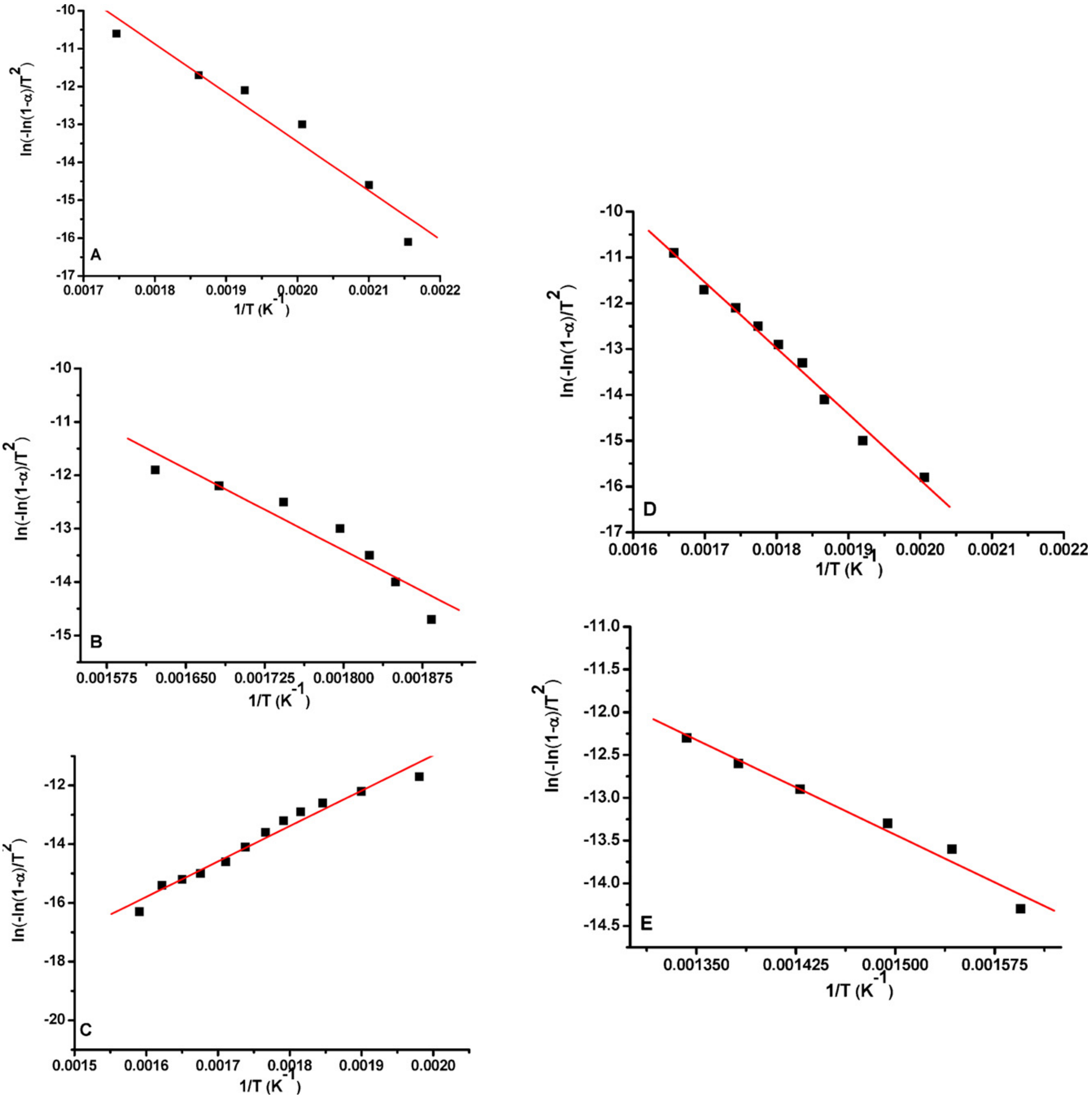

Fig. 7. Coats and Redfern (CR) curves of (A) Cu(II)–H_2L^2, (B) Cu(II)–H_2L^1, (C) Mn(II)–H_2L^2, (D) Mn(II)–H_2L^1 1st, and (E) Mn(II)–H_2L^1 2nd complexes at main decomposition steps.

first decomposition step at 50–217 °C range by estimated mass loss of 23.10 (Calcd. Mass loss 23.68%) and may be attributed to the liberation of coordinated water molecule with C_6H_5O molecule. The rest steps within the temperature range 217–800 °C with an estimated mass loss 48.35 (Calcd. Mass loss 47.53%) may be attributed to the expel of organic molecules. The residual part as MnS polluted with 4C atoms. The TG curve of Cu(II)–H_2L^2 complex was thermally decomposed in five successive decomposition steps. The first estimated mass loss of 2.44% within the range of 46–170 °C may be attributed to the liberation of hydrated molecule (Calcd. Mass loss 2.94%). The second and third steps occur within the range 170–420 °C with an estimated mass loss of 46.83 (Calcd. Mass loss 46.08%) are accounted for the decomposition of $C_{12}H_8 + Cl_2$ and $C_2H_3O_2$ fragments. The fourth and fifth steps occur within the range 420–800 °C with an estimated mass loss of 18.20 (Calcd. Mass loss 18.44%) are accounted for the decomposition of 1.5 N_2 and Cl_2 molecules leaving CuO + CuS polluted with two carbon atoms. The little difference between the estimated mass losses and calculated ones in some decomposition steps may be referring to the interactions happened between the two following steps which may prohibit the distinct identification for the initial and final temperature of the step.

3.9. Kinetic studies

The kinetic parameters such as activation energy (E^*), enthalpy (ΔH^*), entropy (ΔS^*) and free energy change of the decomposition (ΔG^*) were evaluated graphically by employing the Coats–Redfern

Table 5
Kinetic parameters using the Coats–Redfern (CR) equations operated for all complexes.

Complex	Step	Kinetic parameters					
		E (J mol^{-1})	A (S^{-1})	ΔS (J mol^{-1} K^{-1})	ΔH (J mol^{-1})	ΔG (J mol^{-1})	r
(2)	1st	1.20×10^5	1.49×10^9	-7.34×10^1	1.16×10^5	1.52×10^5	0.99421
	2nd	6.16×10^4	1.81×10^2	-2.07×10^2	5.69×10^4	1.72×10^5	0.98835
(3)	3rd	8.49×10^4	3.65×10^5	-1.44×10^2	8.03×10^4	1.59×10^5	0.95225
(5)	2nd	1.00×10^5	1.76×10^{-12}	-4.75×10^2	9.56×10^4	3.59×10^5	0.98412
(6)	2nd	1.07×10^5	7.45×10^8	-7.94×10^1	1.03×10^5	1.43×10^5	0.97344

Table 6
The values of zone inhibition of microorganisms for the ligand and its metal complexes.

Compound	Zone of inhibition (mm)						
	Gram (+) bacteria			Gram (−) bacteria		Fungi	
	Bacillus subtilis	*Streptococcus pneumonia*	*Staphylococcus aureas*	*Escherishia coli* sp.	*Pesudomonas* sp.	*Aspergillus nigaer*	*Penicillium* sp.
(4)	10	6	–	12	8	10	11
(5)	9	9	11	13	–	9	8
(6)	21	23	15	11	20	18	16

relation (Fig. 7) [19]. The equation is a typical integral method, represented as:

$$\int_0^{\alpha} \frac{d\alpha}{(1-\alpha)^n} = \frac{A}{\varphi} \int_{T_1}^{T_2} \exp\left(\frac{-E*}{RT}\right) dt$$

For convenience of integration the lower limit T_1 is usually taken as zero. This equation on integration gives:

$$\ln\left[\frac{-\ln(1-\alpha)}{T^2}\right] = \ln\left(\frac{AR}{\varphi E*}\right) - \frac{E*}{RT}$$

A plot of $\ln[-\ln(1-\alpha)/T^2]$ (LHS) against $1/T$ was drawn. E^* is the energy of activation in J mol^{-1} and calculated from the slop and A is (S^{-1}) from the intercept value. The entropy of activation ΔS^* in (J K^{-1} mol^{-1}) was calculated by using the equation:

$$\Delta S* = R \ln\left(\frac{Ah}{k_B T_s}\right)$$

where k_B is Boltzmann's constant, h is Planck's constant and T_s is the DTG peak temperature.

The calculated values of E^*, A, ΔS^*, ΔH^* and ΔG^* for the decomposition steps are given in Table 5. The most significant results in the considerable higher thermal stability of Mn(II)–H_2L^1 and Cu(II)–H_2L^2 complexes than the Mn(II)–H_2L^2 and Cu(II)–H_2L^2 complexes. The second essential result is the entropy change ΔS^* for the formation of the activated complexes from the starting reactants is in most cases of negative values. The negative sign of the ΔS^* suggests that the degree of structural complexity (arrangement, organization) of the activated complexes was lower than that of the starting reactants and the decomposition reactions are fast [20].

3.10. Antibacterial antifungal activity

The biological activity for H_2L^2 ligand and its two complexes are tested against different organisms as gram-negative, gram-positive and fungi using only one concentration from them in DMF and used as a control. The zone of inhibition against the growth of microorganisms for the compounds is given in Table 6. It has been suggested that the ligand with the N, O and S donor system might have inhibited enzyme production, since enzymes which require free hydroxyl groups for their activity appearance to the especial susceptibility to deactivation by the ions of the complexes. The complexes facilitate their diffusion through the lipid layer of spore membranes to the site of action ultimately killing them by combining with —OH groups of certain cell enzymes. The variation in the effectiveness of different biocidal agents against different organisms depends on the impermeability of the cell. Chelation reduces the polarity of the central metal atom [21], mainly because of partial sharing of its positive charge with the ligand. Also, the normal cell process may be affected by the formation of hydrogen bond, through the azomethine nitrogen atom with the active centers of cell constituents [22]. The chosen compounds used for this investigation are as example only for this study. Also, the absence of bulkiness observed around the metal ions which may permit their interaction easily with the cell enzymes is considered the main cause for the choice. From the results, it is clear that Cu(II)–H_2L^2 complex exhibits inhibition towards all the studied microorganisms and however Mn(II)–H_2L^2 complex exhibits less inhibition. From structure point of view of the prepared compounds with their effects on microbial test. It is clear that the formation of the chelate derived 2:1 molar ratio (M:L) sometimes increase the biological activities of the complex compared to the free ligand. This is may be attributed to the presence of N, O and S groups around the two central atoms arising the inhibition activity of the central atoms which is not the only responsible for the biological activity of its complex. Some metal complexes can enhance the activity and others can reduce this activity with respect to the parent ligand.

Acknowledgements

The authors wish to express many thanks for the Prof. Ibrahim M. El-Deen, Department of Chemistry, Faculty of Science, Port Said University, for his assistant for supported to organic ligands in this study.

References

[1] M.A. Ali, S.E. Livingstone, Coord. Chem. Rev. 13 (1974) 279.
[2] N.K. Singh, A. Srivastava, Trans. Met. Chem. 25 (2000) 133.
[3] M. Wang, L.F. Wang, Y.Z. Ligands, Q.X. Li, Trans. Met. Chem. 26 (2001) 307.
[4] M.X. Li, L.Z. Zhang, D. Zhang, B.S. Ji, J.W. Zhao, Eur. J. Med. Chem. 46 (9) (2011) 4383.
[5] K.M. Vyas, R.G. Joshi, R.N. Jadeja, C.R. Prabha, V.K. Gupta, Spectrochim. Acta A 84 (1) (2011) 256.
[6] M. Belicchi-Ferrai, F. Biscegli, G. Pelosi, S. Pinelli, P. Traascani, Polyhedron 26 (2007) 5150.
[7] A. Majumder, C.R. Chaudrary, S. Mitra, L. Dahlenburg, Struct. Chem. 16 (2005) 611.
[8] A.I. Vogel, A Text Book of Quantitative Inorganic Analysis, Longman, London, 1994.
[9] A.W. Bauer, W.M. Kirby, J.c. Sherris, M. Turck, Am. J. Clin. Pathol. 45 (1966) 493.
[10] N.M. El-Metwaly, Trans. Met. Chem. 32 (2007) 88.

[11] E. Franco, El. Lopez–Trorres, M.A. Mendiola, M.T. Sevilla, Polyhedron 19 (2000) 441.
[12] J.J. Filo, A. Terron, D. Mulet, V. Merno, Inorg. Chim. Acta 135 (1987) 197.
[13] Q. Zhou, T.W. Hambley, B.J. Kennedy, P.A. Lay, P. Turner, B. Warwick, J.R. Biffin, H.L. Regtop, Inorg. Chem. 39 (2000) 3742.
[14] K. Nakamoto, Infrared and Raman Spectra of Coordination Compounds, Wiley-Interscience, New York, 1970.
[15] A.B.P. Lever, Crystal Field Spectra Inorganic Electronic Spectroscopy, 1st ed., Elsevier, Amsterdam, 1968, p. 249.
[16] N.M. Shauib, A.-Z.A. Elassar, A. El-Dissouky, Spectrochim. Acta A 63 (2006) 714.
[17] N.L. Allinger, J. Am. Chem. Soc. 99 (1977) 8127.
[18] HyperChem Professional 7.5, Hypercube, Inc., Gainesville, FL 32601, USA, 2002. Available from: http://www.hyper.com.
[19] A.W. Coats, J.P. Redfern, Nature 201 (1964) 68.
[20] (a) L.T. Valaev, G.G. Gospondinov, Thermochim. Acta 370 (2001) 15;
(b) A.A. Soliman, G.G. Mohamed, Thermochim. Acta 421 (2004) 151.
[21] S.H. Ataiw, A.A. Abou-Hussen, Egypt. J. Chem. 46 (2003) 685.
[22] N. Dharmaraj, P. Viswanathamurthi, K. Natarajan, Trans. Met. Chem. 26 (2001) 105.